Dean&Francis
ISSN 2959-6157

Simulation of Circular Patch Antenna Arrays Corresponding to the 6.6GHz Frequency Band Based on HFSS

Siyuan Wu

Electrical and Electronic Engineering of Southern University of Science and Technology, Shenzhen, China
12212740@mail.sustech.edu.cn

Abstract:

Microwave antennas play a significant role in current wireless communication systems and are key components for converting electromagnetic waves into electrical signals. The performance of the antenna directly affects the distance and quality of the signal transmission. However, antennas still face problems such as high energy consumption, low precision, great integration difficulty, and difficulty in coping with complex environmental conditions that change in real time. This experiment is based on the multi-level simulation optimization technology of HFSS to conduct parametric modeling of circular antennas and optimize the model parameters. Compared with the traditional side-fed circular microstrip patch antenna, this microstrip antenna innovatively adds a groove in the middle of the circular patch. This structure can simultaneously excite the TM11 and TM21 modes, thereby increasing the bandwidth. By optimizing the model parameters, the final frequency band of the antenna can be around 6.6GHz. This project innovatively transformed the single antenna structure into an array form. The final frequency band range can reach 6.36 to 7.04GHz, with a peak gain of 7.5dBi. This scheme provides a simple simulation method for the future microwave antenna engineering.

Keywords: HFSS; microwave; circular microstrip patch antenna.

1. Introduction

The microwave frequency band is one of the most important frequency bands in the field of wireless communication and has extremely wide applications in high-speed communication systems [1]. This frequency band neither has many complex transmission rules like the high-frequency band, nor is it as fiercely competitive in terms of spectrum as the low-frequency band. Meanwhile, compared with the low-frequency band, the microwave frequency band has a wider continuous spectral bandwidth. For example, for the 100MHz bandwidth defined by 5G NR, when deployed in the 3.5GHz frequency band,

ISSN 2959-6157

the theoretical peak rate can reach 1.4Gbps, while the same bandwidth can only achieve a rate of approximately 300Mbps in the 800MHz frequency band. This is mainly because the microwave frequency band can use many complex modulation methods such as 256QAM [2].

To give full play to these advantages of the microwave frequency band in high-speed communication, antennas capable of transmitting and receiving microwave signals are particularly important. In order to significantly reduce the design cost of antennas, simulation is widely applied in the design of antennas. With the increasingly complex development of antenna structure, the traditional antenna design method based on empirical formulas has been difficult to meet the performance requirements, and full-wave electromagnetic simulation software such as HFSS, CST, and FEKO is becoming indispensable tools. These software can accurately simulate the radiation characteristics of antennas in the microwave frequency band and calculate the propagation loss in complex electromagnetic environments by solving Maxwell‘s equations. Especially when dealing with miniaturized antennas and dense arrays, simulation software can reveal subtle electromagnetic phenomena that are difficult to capture through traditional theoretical analysis, such as the influence of dielectric loss on radiation efficiency and key parameters like the mutual coupling effect between elements. Through parametric modeling and optimization algorithms, engineers can quickly verify various innovative designs in a virtual environment, significantly shortening the development cycle from concept to product.

HFSS, CST and FEKO, as three mainstream electromagnetic simulation software, each have their own characteristics. HFSS, based on the Finite element method (FEM), is particularly adept at handling high-precision issues. CST employs the finite time-domain integration (FIT) method, which demonstrates high efficiency in wideband time-domain analysis and regular structure simulation [3]. FEKO takes the method of Moments (MoM) as its core and combines it with high-frequency approximation methods.

The time-domain solver of CST can obtain the wibroadband response through a single simulation, which is highly efficient in high-speed digital circuits and transient electromagnetic compatibility analysis. However, its adaptability to curved surface structures is not as flexible as that of HFSS. FEKO, with its surface integral equation and hybrid algorithm, can handle large-sized problems with low memory usage [4]. However, its accuracy will significantly decline when dealing with scenarios where the medium is non-uniform or the volume mesh needs to be discrete. Overall, although the full-wave finite element method of HFSS consumes a large amount of computing resources, its analysis results are also the most accurate. It has intuitive and accurate results when dealing with high-frequency problems and exploring the mutual influence between elements, such as mutual coupling effects.

This project gives full play to the performance advantages of HFSS, conducts parametric modeling of the circular patch antenna, and optimizes the parameters of the model individually and jointly, thereby obtaining an antenna operating at 6.6GHz. Moreover, it innovates and transforms it into the form of an array antenna, and optimizes some parameters so that its performance remains unchanged compared to a single antenna unit.

2. Key Technologies for Optimizing HFSS Microwave Antennas

2.1 Parametric Modeling and Optimization

Parametric modeling and optimization are the primary steps in the design of HFSS antennas, with the core being the establishment of a mathematical correlation between geometric parameters and electromagnetic performance [5]. Designers can build parametric geometry models by defining key size variables such as surface mount size, feed position, dielectric thickness, etc. The parameter scanning function provided by HFSS can systematically and intuitively study the influence of each parameter on performance indicators such as S-parameters and gain, and draw images. In terms of optimization algorithms, HFSS has proposed various methods such as gradient optimization and genetic algorithms. For example, in the design of microstrip antennas, the resonant frequency f_r can be precisely controlled by parametrically adjusting the edge length of the circular patch. During the optimization process, HFSS will automatically calculate the sensitivity of the objective function (such as S11 bandwidth ≤-10dB) to each parameter to guide the direction of the design iteration. Practice shows that, compared with the traditional trial-and-error method, this parameter optimization method based on the actual model has obvious improvements.

2.2 Adaptive Grid Encryption Technology

Adaptive grid encryption technology is the core technology for HFSS to ensure simulation accuracy [6]. This technology automatically identifies areas with drastic field changes (such as the edge of the patch and near the power supply point) for local grid subdivision through iterative solution and error estimation. In the design of millimeter-wave antennas, the working wavelength may only be 3-5mm, and the mesh size is required to reach λ/10 or even smaller. HFSS uses high-order basis functions (sec-

ond-order or third-order vector elements) to describe the field distribution. Compared with the traditional first-order elements, it can improve the calculation accuracy by an order of magnitude under the same grid density. The adaptive process usually involves 4 to 6 rounds of iterations. If the results do not converge after the iterations, the software will issue a warning. In the software, the number of iterations can be increased by itself. Each round, the mesh is adjusted based on the residual distribution of the previous solution until the convergence criterion is met. This intelligent grid strategy can not only ensure the resolution of key areas, but also avoid the computational waste caused by global excessive discretization.

2.3 High-performance Computing Acceleration Technology

High-performance computing acceleration technology has greatly enhanced the optimization efficiency of large-scale antenna arrays [7]. The Domain Decomposition method (DDM) adopted by HFSS divides the computing domain into multiple sub-regions and processes them in parallel through distributed memory. For the 256-element phased array simulation, the adoption of 32-core parallelism can reduce the solution time from 72 hours to 4 hours. The GPU acceleration technology introduced in recent years is particularly suitable for the matrix solution link in the finite element method, and an acceleration ratio of 5 to 8 times can be achieved on the NVIDIA A100 graphics card. HFSS has also developed a hybrid basis function technology, using low-order elements in smooth areas and high-order elements in detailed areas to further balance accuracy and speed. For the frequency sweep requirements, wideband fast frequency sweep techniques (such as adaptive sampling interpolation) only need to calculate 3 to 5 characteristic frequency points to accurately reconstruct the entire frequency band response.

2.4 The Multi-physics Field Cooperative Optimization Technology

The multi-physics field cooperative optimization technology achieves precise prediction and optimization of antenna performance in the actual working environment by establishing the coupling relationship among multiple physics fields such as electromagnetic, thermal and structural ones [8]. This technology utilizes the deep integration of HFSS with simulation tools such as thermal analysis and structural mechanics to construct a complete multi-field coupling analysis process. In terms of electromagnetic-thermal coupling, the system first calculates the electromagnetic loss distribution of the antenna when it operates at high power. Then, these losses are introduced as heat sources into the thermal analysis software to simulate the variation process of the temperature field. Finally, the temperature distribution is fed back to the electromagnetic model to analyze the influence of material parameter changes on the antenna performance and form a closed-loop optimization. For the structure-electromagnetic coupling problem, the deformation of the antenna under mechanical load is obtained through fluid-structure coupling analysis. Then, the geometric model after deformation is re-imported into the electromagnetic simulation to evaluate the influence of structural deformation on the radiation characteristics. This multi-physics field iterative optimization method breaks the limitations of traditional single-field analysis, expanding antenna design from simple electromagnetic performance optimization to comprehensive design including engineering factors such as thermal management and structural reliability, significantly enhancing the working stability of the product in actual complex environments. By establishing parametric correlation models among various physical fields, engineers can systematically evaluate the comprehensive performance of different design schemes under multiple working conditions, thereby finding the optimal balance point.

2.5 Machine Learning-assisted Optimization Technology

Machine learning-assisted optimization technology represents a new paradigm in antenna design. HFSS integrates Python API to support interaction with frameworks such as TensorFlow/PyTorch and build intelligent optimization processes. Deep neural networks can establish proxy models of design parameters (input layer) and performance indicators (output layer) to replace part of the full-wave simulation [9]. Experiments show that the proxy model trained with 500 groups of samples can control the error of predicting S11 within 1dB, and the evaluation time is only 1/1000 of the full simulation of HFSS. Reinforcement learning algorithms are used for formulating optimization strategies, such as automatically adjusting the crossover rate and mutation rate of genetic algorithms. In the design of 5G millimeter-wave lens antennas, machine learning-assisted optimization found the optimal solution that traditional methods would require 2,000 iterations in just 200 iterations, with a significant improvement in efficiency. It should be noted that the accuracy of the proxy model depends on the coverage of the training samples and usually requires the dynamic expansion of the dataset in combination with active learning strategies.

3. Simulation Case: Simulation of Cir-

ISSN 2959-6157

cular Patch Antenna Array

3.1 Simulation of Antenna Units

3.1.1 Theoretical basis

The radius of the circular patch is given by the following two formulas [10].

$$a = \frac{F}{\sqrt{1+\frac{2h(cm)}{\pi \delta_r F}\left[ln\frac{\pi F}{2h(cm)}+1.7726\right]}}(cm) \quad (1)$$

$$F = \frac{8,791\times10^9}{f_r\sqrt{\delta_r}} \quad (2)$$

Where a is the radius of the circular patch. h represents the thickness of the dielectric substrate (unit: centimeters), δ_r is the relative dielectric constant of the dielectric, and f_r is the resonant frequency (unit: Hertz).

3.1.2 Parametric modeling

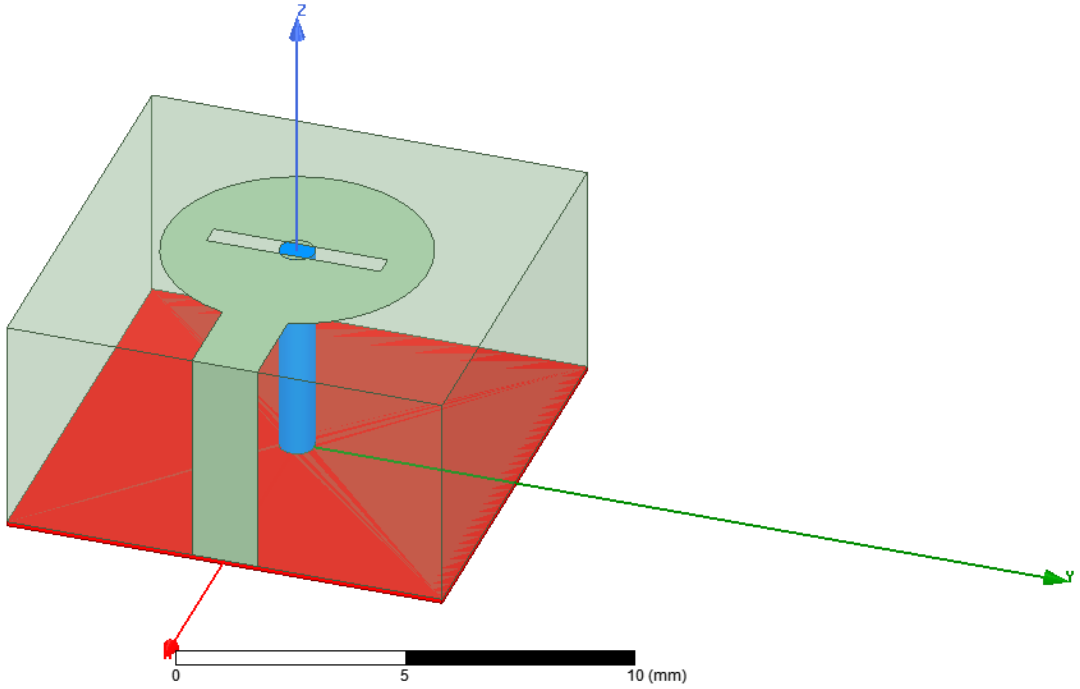

Fig. 1 Modeling of circular patch antennas

Table 1. The relevant parameters of the model

Name	Value	Unit	Evaluated Value
wsub	10	mm	10mm
lsub	10	mm	10mm
hsub	5	mm	5mm
rp	3	mm	3mm
wf100	1.5	mm	1.5mm
lf	2.1	mm	2.1mm
wc	0.5	mm	0.5mm
lc	4	mm	4mm
t	0.1	mm	0.1mm

In table 1, wsub is the width of the dielectric substrate, lsub is the length of the dielectric substrate, hsub is the thickness of the dielectric substrate, rp is the radius of the circular patch antenna, wf100 is the width of the trans-

mission line, lf is the length of the transmission line, wc is the width of the rectangular slot, lc is the length of the rectangular slot, and t is the thickness of the grounding base plate, which is a copper plate. The feeder under the rectangular groove is a copper cylinder with a radius of 0.4mm. The model is fed in the form of lumped ports. The dielectric substrate adopts Rogers RT/duroid 5880(tm) material with a dielectric constant of 2.2, dielectric Loss Tangent of 0.0009. Fig. 1 shows the specific model [11].

3.1.3 Parameter sensitivity analysis

Scan parameters for rp:

Fig. 2 The relationship between rp and S11

The radius of the circular patch antenna is inversely proportional to the resonant frequency, and this correlation stems from the propagation characteristics of electromagnetic waves in the medium. When the antenna radius decreases, the propagation path of electromagnetic waves in the dielectric substrate shortens, resulting in a corresponding reduction in the wavelength required for resonance. Since frequency is inversely proportional to wavelength, the frequency will increase as fig. 2. Meanwhile, the thickness and dielectric constant of the dielectric substrate also affect this relationship - a thicker substrate or a higher dielectric constant will enhance the confinement effect of the electromagnetic field, making the trend of frequency increase more obvious in the case of small radii. The logarithmic term reflects the correction effect of the edge electromagnetic field. This edge effect is particularly significant in small-sized antennas, further enhancing the frequency increase effect brought about by the reduction in radius. Overall, by adjusting the combination of these parameters, precise control of the antenna‘s operating frequency can be achieved.

Scan parameters for lc:

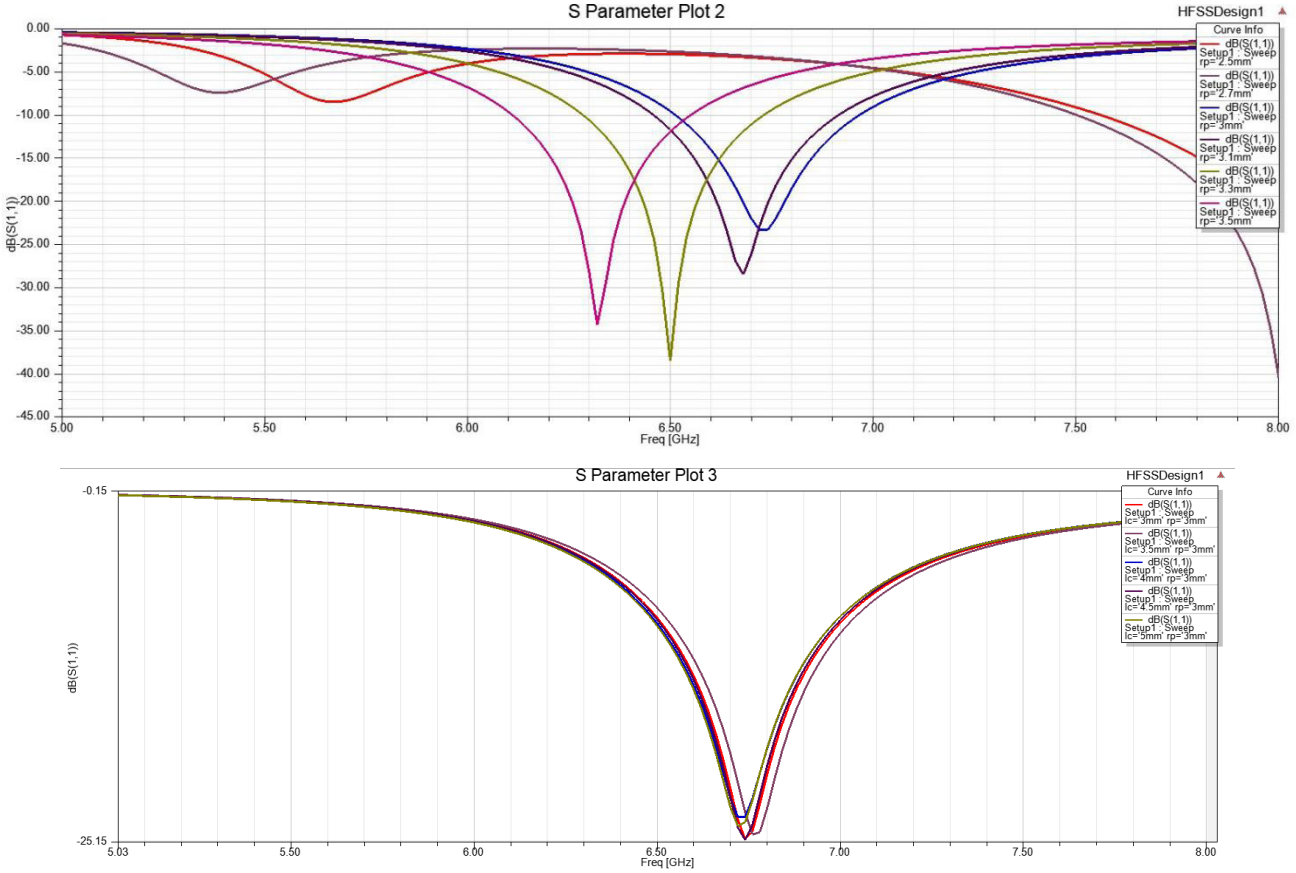

Fig. 3 The relationship between lc and S11

Similarly, the influence of the aperture width can also be obtained. Through fig. 3, it can be found that the size of the aperture basically does not affect the position of the frequency band.

3.2 The combination of antenna arrays

3.2.1 Parallel connection of antenna units

If the antenna units are to be arranged in an array form and the default input impedance during power supply is 50 ohms, then if the two antennas are connected in par-

ISSN 2959-6157

allel, the input impedance of each antenna unit should be 100 ohms. Therefore, the width of the wf100 should be adjusted first to make its input impedance reach 100 ohms. Then the antenna units are replicated so that the distance between the centers of the two antenna units reaches half of the working wavelength.

Because when the unit spacing exceeds λ/2, the array pattern will show periodically repetitive gate lobes [12] [13]. The spacing of λ/2 can ensure that only one main lobe appears within the visible Angle range. Secondly, this spacing can also effectively suppress the mutual coupling effect. A spacing that is too small will significantly increase the electromagnetic coupling between units, leading to impedance mismatch and a decrease in radiation efficiency. The spacing of λ/2 can achieve a good balance between suppressing mutual coupling and maintaining the compactness of the array, and usually the mutual coupling can be controlled below -15dB. Finally, the λ/2 spacing provides the optimal beam resolution for the array. For a linear array containing N elements, this spacing can generate a beam width of approximately 2arcsin(2/N), ensuring sufficient gain while taking into account good angular resolution.

Then, connect the two antenna units together with a 100-ohm microstrip line. Finally, feed the entire antenna array with a 50-ohm microstrip line in the middle of the two units. Through these operations, a single antenna was successfully converted into an array form.

3.2.2 The simulation results of the array antenna are presented

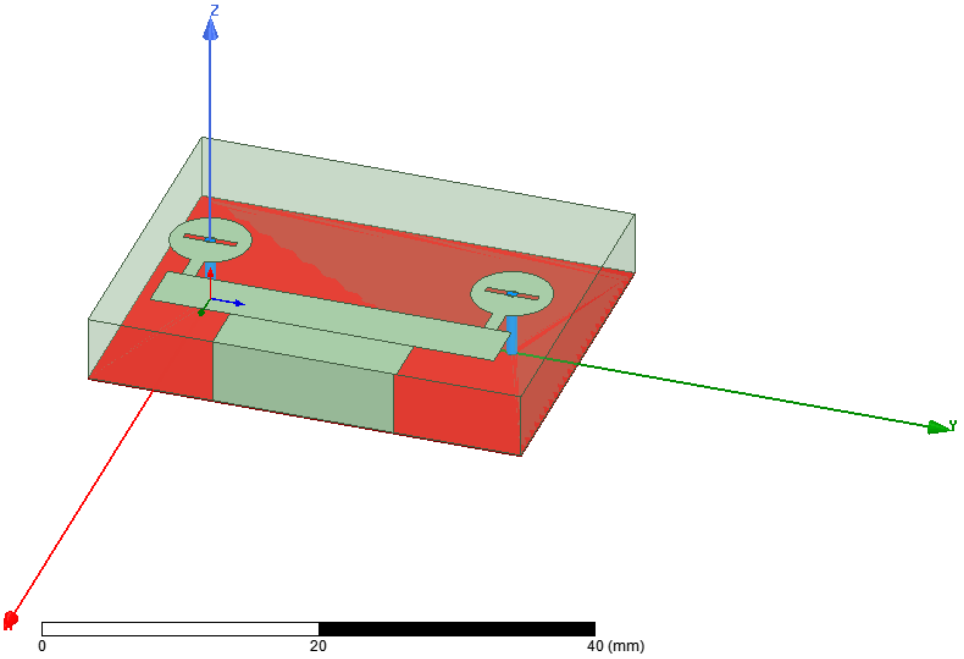

Fig. 4 Simulation model of array antenna

Table 2. Parameters of the array antenna

Name	Value	Unit	Evaluated Value
lsub	10	mm	10mm
wsub	26	mm	26mm
hsub	5	mm	5mm
wf100	1	mm	1mm
lc	4	mm	4mm
lf	2.1	mm	2.1mm
rp	3	mm	3mm
wc	0.5	mm	0.5mm

t	0.1	mm	0.1mm
ll100	4	mm	4mm
wl100	3.2	mm	3.2mm
ll50	4	mm	4mm

The newly added wl100 is the width of the 100-ohm microstrip line, ll100 is the length of the 100-ohm microstrip line, ll50 is the length of the 50-ohm microstrip line as table 2, and the width of the 50-ohm microstrip line is 13.8mm. Fig. 4 shows the specific model.

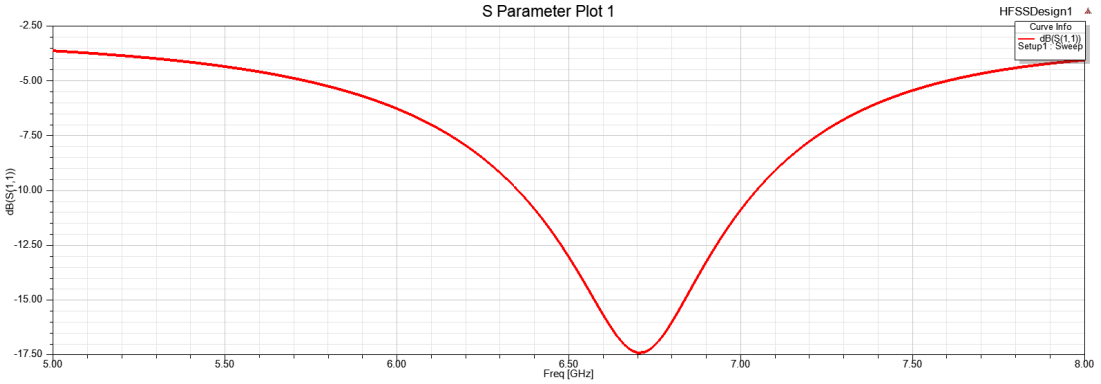

Fig. 5 S11 parameter diagram

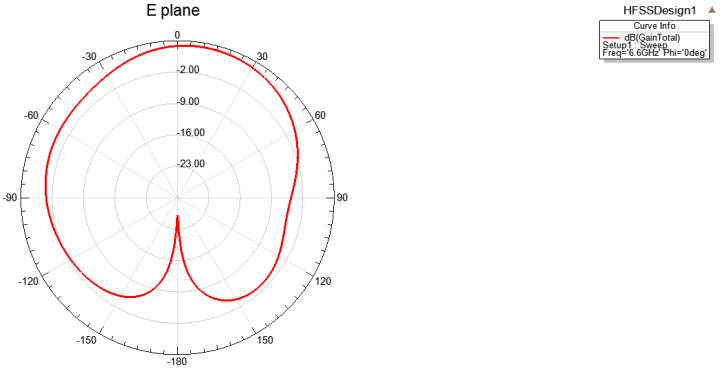

Fig. 6 E-Plane Gain Pattern

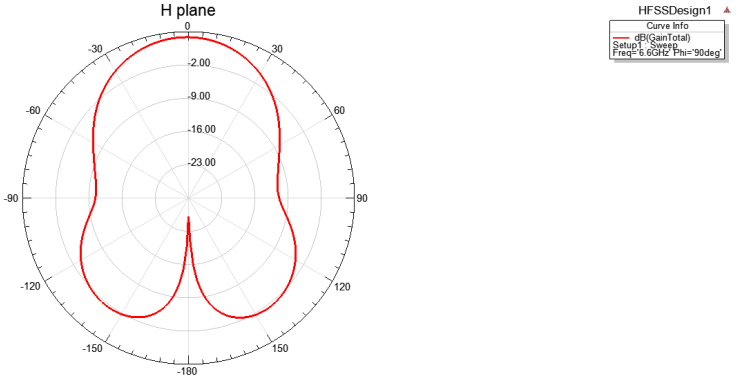

Fig. 7 H-Plane Gain Pattern

The phase frequency band of the array antenna is shown in fig. 5, which is 6.36 to 7.04GHz, slightly expanded compared with the single antenna. However, when the frequency is 6.5 GHz, the minimum reflection coefficient S11 only reaches -17.4dB, which is significantly lower compared to a single antenna. Meanwhile, by observing

ISSN 2959-6157

the gain plots of the E-plane and H-plane as shown in fig. 6 and fig. 7, it can be found that the side lobe level of the H-plane gain plot is less than -12 dB. Therefore, there may be a slight coupling effect.

4. Conclusion

Since the finite element method of HFSS makes the calculation more accurate, this project conducts parametric modeling and optimization of a small circular microstrip patch antenna based on HFSS, and improves it into an array form. Based on the flexibility of microstrip patch antennas and their ease of integration into arrays, in the later stage, the working frequency band of the antenna can be adjusted by changing the radius of the circular microstrip patch, or more antenna units can be integrated by modifying the width of the microstrip line.

In addition, some methods can be adopted to optimize the mutual coupling effect. The cell spacing can be optimized (usually greater than half the wavelength to reduce near-field coupling), decoupling structures (such as defect ground structure DGS or electromagnetic band gap EBG) can be adopted, orthogonal polarization or differentiated radiation modes can be designed to reduce energy interaction, non-uniform array layouts (such as random distribution) can be used to disrupt periodic coupling, and matching networks can be introduced to compensate for impedance mismatch caused by coupling. In addition, the application of amplitude/phase weighting (such as Taylor distribution) in the feed design can suppress sidelobe coupling.

References

[1] D. He et al., „Channel Measurement, Simulation, and Analysis for High-Speed Railway Communications in 5G Millimeter-Wave Band," in IEEE Transactions on Intelligent Transportation Systems, vol. 19, no. 10, pp. 3144-3158, Oct. 2018, doi: 10.1109/TITS.2017.2771559.

[2] J. Yang, H. Zhao, W. Wang and C. Zhang, „An effective SINR mapping models for 256QAM in LTE-Advanced system," 2014 IEEE 25th Annual International Symposium on Personal, Indoor, and Mobile Radio Communication (PIMRC), Washington, DC, USA, 2014, pp. 343-347, doi: 10.1109/PIMRC.2014.7136187.

[3] K. Luo, S. -H. Ge, L. Zhang,et al. „Simulation Analysis of Ansys HFSS and CST Microwave Studio for Frequency Selective Surface," 2019 International Conference on Microwave and Millimeter Wave Technology (ICMMT), Guangzhou, China, 2019, pp. 1-3, doi: 10.1109/ICMMT45702.2019.8992280.

[4] M. Márton, L. Ovseník, J. Turán, et al. „Design of Microstrip Patch Antennas Operating on 2.45 GHz in HFSS and FEKO," 2019 IEEE 15th International Scientific Conference on Informatics, Poprad, Slovakia, 2019, pp. 000421-000426, doi: 10.1109/Informatics47936.2019.9119331.

[5] Z. Ye, W. Shao, X. Ding et al., „Automatic Sampling Scheme in Parametric Modeling of Microwave Antennas," 2020 International Conference on Microwave and Millimeter Wave Technology (ICMMT), Shanghai, China, 2020, pp. 1-3, doi: 10.1109/ICMMT49418.2020.9386795.

[6] L. Gan, W. Jiang, Q. Chen, et al. „Method to Estimate Antenna Mode Radar Cross Section of Large-Scale Array Antennas," in IEEE Transactions on Antennas and Propagation, vol. 69, no. 10, pp. 7029-7034, Oct. 2021, doi: 10.1109/TAP.2021.3075536.

[7] L. Shen, P. Jia, X. Yang,et al. „FEM-BEM-DDM for Electromagnetic Radiation Analysis of Periodic Antenna Array," 2020 International Conference on Microwave and Millimeter Wave Technology (ICMMT), Shanghai, China, 2020, pp. 1-3, doi: 10.1109/ICMMT49418.2020.9386657.

[8] Z. Chen, H. Bayat and A. Adhyapak, „Multiphysics Analysis of RF Pyramidal Absorbers," 2019 Antenna Measurement Techniques Association Symposium (AMTA), San Diego, CA, USA, 2019, pp. 1-6, doi: 10.23919/AMTAP.2019.8906386.

[9] M. Devnath, P. Ranjan and R. Chowdhury, „A Dual-Band Millimeter Wave Cylindrical Dielectric Resonator Antenna Using Machine Learning Approach," 2024 IEEE International Conference on Interdisciplinary Approaches in Technology and Management for Social Innovation (IATMSI), Gwalior, India, 2024, pp. 1-5, doi: 10.1109/IATMSI60426.2024.10503490.

[10] Balanis, Constantine A. Antenna Theory: Analysis and Design. 3rd ed. Hoboken, NJ: John Wiley, 2005.

[11] V. S. Vamsi, B. Panda and K. R. Subhashini, „Design and Analysis of Slotted circular patch Antenna for Wi-Fi Applications," 2022 IEEE Wireless Antenna and Microwave Symposium (WAMS), Rourkela, India, 2022, pp. 1-3, doi: 10.1109/WAMS54719.2022.9848283.

[12] G. S. Shravan, L. Sai Suhas, N. G. Hemanth Kumar, et al. „2x2 Circular Patch Antenna Array at 2.4 GHz for WSN Applications: Design and Performance Analysis of Circular Antenna Array and Comparison over Rectangular Array," 2019 International Conference on Communication and Electronics Systems (ICCES), Coimbatore, India, 2019, pp. 887-891, doi: 10.1109/ICCES45898.2019.9002605.

[13] O. S. Baskoro, I. P. Ardana, P. K. Sudiarta et al, „A 2×2 Inset Feed Circular Patch Antenna Array for 1.8GHz LTE Application," 2018 4th International Conference on Wireless and Telematics (ICWT), Nusa Dua, Bali, Indonesia, 2018, pp. 1-4, doi: 10.1109/ICWT.2018.8527823.